

## Short Communication

# Ag-Conjugated Nanoparticle Biosynthesis Mediated by Rosemary Leaf Extracts Correlates with Plant Antioxidant Activity and Protein Content

Mojtaba Hadi Soltanabad<sup>1</sup>, Mohammad B. Bagherieh-Najjar<sup>1,\*</sup>,  
Eisa Kohan Baghkheirati<sup>1,2</sup> and Manijeh Mianabadi<sup>1</sup>

<sup>1</sup>Department of Biology, Golestan University, Shahid Beheshti Ave., P. O. Box: 155, Gorgan, I. R. Iran.

<sup>2</sup>Department of Biology, Hakim Sabzevari University, P. O. Box: 397, Sabzevar, I. R. Iran.

(\*) Corresponding author: mb.bagherieh@gu.ac.ir

(Received: 14 January 2017 and Accepted: 17 July 2017)

### Abstract

In recent years, the world has witnessed an explosion of interest in biogenic synthesis of metallic nanoparticles (NPs), using plant extracts; however, the plant constituents involved in this reaction are poorly characterized. Here, major components of Rosemary (*Rosmarinus officinalis* L.) leaf extracts were isolated monthly during 2012-2013 and their competences for Ag-conjugated nanoparticle biosynthesis were studied. Formation of Ag/AgCl-NPs was examined using UV-visible spectroscopy and characterized by Fourier transform infrared spectroscopy (FTIR), X-ray powder diffraction (XRD), and Transmission electron microscopy (TEM). Correlation analysis showed that extracts with more protein contents and higher total reducing capacity were more efficient in biosynthesis of Ag/AgCl-NPs. There existed no correlation between total phenolic, ascorbic acid and anthocyanin contents with Ag/AgCl-NPs biosynthesis activity. These results partly explain the mechanisms controlling plant mediated biosynthesis of nanoparticles, with possible applications in standardization of plant materials harvested throughout a year.

**Keywords:** Ag/AgCl-NPs Biosynthesis, Antioxidant Activity, FTIR, Nanoparticles, *Rosmarinus Officinalis*.

## 1. INTRODUCTION

Among various metallic nanoparticles (NPs), Ag-conjugated NPs are especially important because of their wide range of applications in various fields [1]. Recently, efforts have been directed towards biogenic synthesis of metallic nanoparticles (NPs) mediated by plant extracts, due to their lower costs, high rate of synthesis and production of fewer by-products [2-5]. To comprehend the mechanisms governing bio-reduction of Ag<sup>+</sup> ions into nanoparticles, it is useful to identify plant ingredients playing vital roles in the reaction, and

to analyze their environmentally driven seasonal fluctuations.

Results obtained from biogenic synthesis of NPs mediated by various plant extracts, including Rosemary (*Rosmarinus officinalis*) leaf extracts [6-8] suggest that plants with higher antioxidant activities are better sources for green synthesis of metallic NPs although, little is known about the exact plant constituents involved in this reaction. Here we aimed to evaluate the contents of phenolics, flavonoids and antioxidant activity of Rosemary leaf extracts prepared from plants in various seasons

and to examine their ability in biogenic synthesis of NPs. The data show that Rosemary leaf extracts harvested in various seasons exhibit quite different abilities for biosynthesis of Ag-conjugated nanoparticles. Furthermore, new means towards understanding the mechanisms that control biogenic synthesis of NPs by plant extracts has been proposed.

## 2. MATERIALS AND METHODS

The leaves of *R. officinalis* L. collected from Golestan University campus, Gorgan, Iran (54°25'E; 36°50'N) during 2012-2013, were briefly washed with distilled water, air dried at 50 °C for 48 h and ground to a fine powder, using a cutting mill. 1 g of dry rosemary leaves powder was extracted in 50 ml of 95% ethanol for 48 hours, at room temperature.

For biogenic synthesis of Ag-conjugated NPs, 1% (V/V) of the plant extract and 1 mM of AgNO<sub>3</sub> (Sigma-Aldrich, Germany) were mixed and retained at room temperature for 0, 45, 90, 150, 210 or 300 min. The solutions were then centrifuged at 20,000g for 15 min and the resulting pellet was washed two times with distilled water and were left at room temperature for 16 h to dry before further characterizations.

The progress of Ag/AgCl-NPs was monitored by measuring changes in the solution color, using a UV-Vis spectrophotometer (Shimadzu UV-1800, Japan) in the range of 200 to 800 nm. A mixture of the nanoparticle powder and KBr was ground into a fine powder and pressed to form a pellet. FTIR was performed using the Spectrum RXI instrument (PerkinElmer, USA) in the range of 4000-400 cm<sup>-1</sup> at a resolution of 4 cm<sup>-1</sup> as described by the supplier. The crystallite structure of the particles was determined by recording their elemental spectra by an X-ray diffractometer (D<sub>8</sub>-Advance, Bruker, Germany) equipped with a CuK $\alpha$  radiation source ( $\lambda$ = 1.54 Å) in the range of 20° to 80° at a 0.5 degree/s scan rate. The average crystallite size of the nanoparticles was estimated by

Sherrer's formula ( $D = 0.9\lambda/\beta \cos\theta$ ), where  $\lambda$  stands for the X-ray wavelength,  $\beta$  for the full width at half-maximum and  $\theta$  for the diffraction angle. The data were analyzed by the X Powder software package. The shape and size of the synthesized nanoparticles were examined by a Philips CM120 transmission electron microscope at 120 kV with a 2.5 Angstrom resolution, as described by the supplier.

FRAP (Ferric reducing antioxidant power) were measured based on the formation of a blue complex [Fe<sup>2+</sup>/TPTZ (2, 4, 6-tripyridyl-s-triazine)]. For this assay, 4.5 mL of FRAP reagent (Sigma-Aldrich, Germany), 450 mL double distilled water, and 150 mL of the plant sample were mixed and incubated in the dark for 30 min at room temperature. Formation of the blue complex was measured by spectrophotometry (Shimadzu UV-1800, Japan) at 593 nm and expressed as mmol Fe<sup>2+</sup>/(g dry wt), using a standard curve of ferrous sulfate [9].

The ability of the rosemary leaf extracts to scavenge DPPH free radicals was measured by ascorbic acid standard curve. The absorbance was spectrophotometrically measured at 517 nm (Shimadzu UV-1800, Japan) after 30 minutes and the percentage of inhibition activity was calculated according to Equation 1.

$$\% I = \frac{(A_0 - A_1)}{A_0} \times 100 \quad \text{Equation 1}$$

Where, % I is the inhibition percentage of DPPH radicals; A<sub>0</sub> is the absorbance of the blank sample and A<sub>1</sub> is the absorbance of the extracts. According to the % I curve, IC<sub>50</sub> (concentration of extracts that reduce 50% of DPPH radicals) was calculated using linear regression analysis. Low IC<sub>50</sub> indicates a high radical-scavenging activity. The results were expressed as ascorbic acid equivalent antioxidant activity (AEAC) [10].

Total phenolic content of extracts were measured using Folin-Ciocalteu test, as described by Meda, et al. [11]. Briefly, two ml of 2 % sodium carbonate (Na<sub>2</sub>CO<sub>3</sub>), 2.8 ml distilled water and 100  $\mu$ l of 50 % (v/v)

aqueous Folin-Ciocalteu's reagent (Merck, Germany) were added to 100  $\mu$ l of the extract. Absorption was measured at 720 nm (Shimadzu UV-VIS, Japan) after 30 min incubation in the dark at room temperature and the results were expressed as milligram Gallic acid equivalent (GAE)/(g dry wt).

Total flavonoid content of the extracts was determined using the aluminum chloride colorimetric method, as described by Chang, et al. [12]. The same procedure was applied to obtain a standard curve using standard quercetin solutions (20–200 mg/l). The data were expressed as milligram quercetin equivalent (QE)/(g dry wt). The ascorbic acid (AA) content was determined by 2, 6-dichlorophenolindophenol-dye method, as described by De Pinto, et al. [13] and was expressed as mg ascorbic acid/(g dry wt).

Total anthocyanin was measured according to Mita et al [14]. For this measurement, 0.02 g of dried plant tissue and 4 ml of methanol containing 1% HCl were pulverized in a porcelain mortar. The mixture was kept at 4 °C for 24 hours and centrifuged for 10 min at 14000 g. Then, absorption of supernatant was measured at 530 and 657 nm. Anthocyanin level for each extract was calculated using Equation 2.

$$\text{Abs} = \text{Abs}_{530} - (0.25 \times \text{Abs}_{657})$$

Equation 2

Where, Abs indicates the absorption (subscripts numbers in the measured wavelength).

The soluble sugar was assayed using the phenol-sulfuric acid method [15]. 0.05 g of dried powdered leaves was added to a test tube containing 5 ml 70% (V/V) ethanol and incubated at 4 °C for one week. Then, the extract was centrifuged for 15 min at 10000 g at room temperature. 0.5 ml of the supernatant was decanted in test tube and was diluted to 2 ml using distilled water, then 1 ml concentrated sulfuric acid and 5 ml of 5% phenol were added to each test tube. After keeping the mixture at room temperature for 30 min the absorption

was measured at 485 nm. The results were expressed as milligram glucose equivalent/(g dry wt).

Soluble protein content was measured according to the Bradford method [16]. For preparation of the Bradford reagent 100 mg Coomassie Brilliant Blue G-250 was dissolved in 50 ml of 95% ethanol, and was added to 100 ml of 85% (w/v) phosphoric acid. After dissolving the dye, the solution was diluted to 1 liter with deionized water and filtered through Whatman No. 3 paper just before use. To measure the soluble protein, 50  $\mu$ l of extracts was diluted to 100  $\mu$ l with distilled water and 5 ml of Bradford reagent were added to each sample. After vortex, samples were incubated at room temperature for 15 min and their absorptions were measured at 595 nm (Shimadzu UV-VIS, Japan). The soluble protein content of the extracts was reported as microgram albumin equivalent/(g dry wt).

Antimicrobial activity of synthesized Ag/AgCl-NPs was evaluated against *Escherichia coli* as a Gram-negative and *Staphylococcus aureus* as a Gram-positive bacterium, using standard Kirby-Bauer disc diffusion method. The bacterial suspensions were swabbed on Muller Hinton Agar. Sterile discs (6 mm  $\Phi$ ) supplemented with or without 30  $\mu$ g Ag/AgCl-NPs, were placed on inoculated growth media, to test bacterial growth. Amikacin (30  $\mu$ g) was used as positive control. After 24 h of incubation at 37 °C, bacterial growth inhibition was determined as diameter of the inhibition zones around the discs.

All experiments were performed at least in triplicate and the data were shown as mean  $\pm$  standard errors (SE). Analysis of variance (ANOVA), Duncan test and Pearson's correlation were used for statistical analyses at  $P \leq 0.05$  confidence level.

### 3. RESULTS AND DISCUSSION

Formation and gradual accumulation of synthesized nanoparticles were confirmed by UV-vis spectroscopy. Reduction of  $\text{Ag}^+$  to Ag-conjugated NPs was moni-

tored by the color change of the solution from yellow to dark brown (Figure 1a). The TEM image of the presumably synthesized Ag-conjugated NPs, indicated that the synthesized nanoparticles were 4-14 nm spheres with an average of 12.5 nm (Figure 1b).

The X-ray diffraction (XRD) spectrum confirmed the crystalline nature of the particles, with reflecting peaks at  $2\theta$  values of

$27.8^\circ$ ,  $32.3^\circ$ ,  $46.5^\circ$ ,  $54.8^\circ$ ,  $57.4^\circ$  and  $76.2^\circ$  corresponding to the (111), (200), (220), (311), (222) and (420) crystal planes of the face-centered cubic (FCC) AgCl (ICDD file no. 00-001-1013). Besides, there existed four diffraction peaks appearing at  $2\theta$  values of  $38.1^\circ$ ,  $44.1^\circ$ ,  $64.2^\circ$ , and  $77.6^\circ$  corresponding to the (111), (200), (220), and (311) crystal planes of FCC Ag (ICDD file no. 00-087-0718) (Figure 1c).

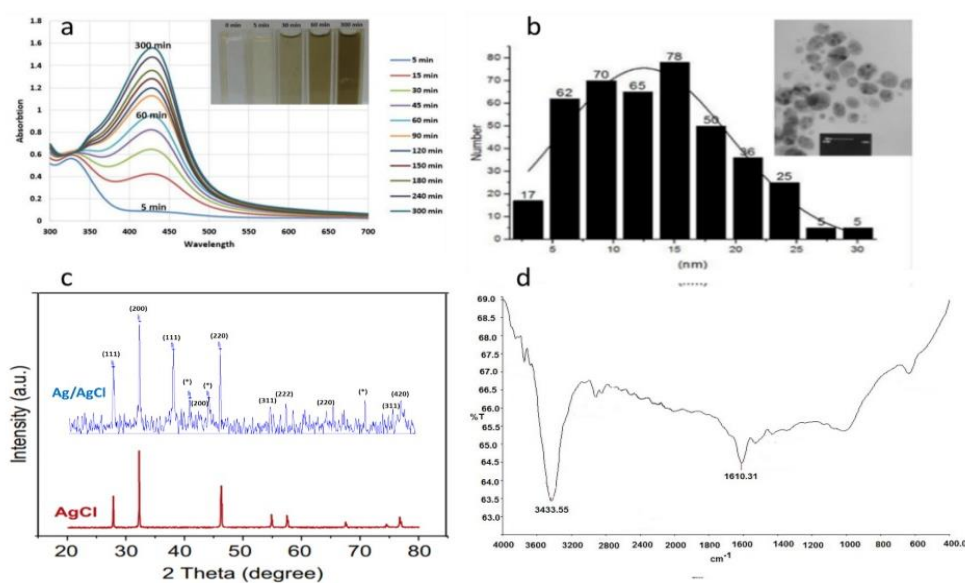


**Figure 1.** (a) UV-Vis spectrum of Ag/AgCl-NPs synthesized. The color change of reaction mixtures is depicted on the graph; (b) TEM image and histogram estimation of particle sizes of the TEM images; (c) X-ray diffraction pattern. (a.u. = arbitrary units). (\*) attributed to the diffraction peaks of additional plant derived compounds are attached to the surface of synthesized Ag/AgCl-NPs; (d) The FTIR spectrum of the synthesized nanoparticles.

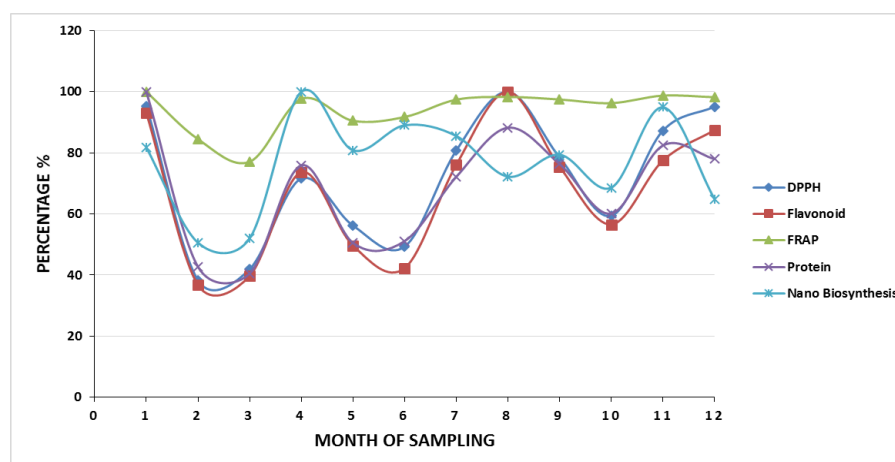


**Figure 2.** Correlation between total phenolic content (TPC), total flavonoid, FRAP and DPPH radical-scavenging activity with Ag/AgCl-NPs synthetic potential of ethanolic leaf extracts of rosemary across various months of a year.

These data indicated that a mixture of Ag/AgCl NPs were synthesized in our reaction. Presence of AgCl NPs indicated that the chlorine ions readily reacted with the AgNO<sub>3</sub> to form Ag/AgCl nanoparticles. A few unassigned diffraction peaks might be related to the crystallization of organic phases that attached to the surface of synthesized Ag/AgCl-NPs [17]. This data is consistent with previously published manuscripts explaining green synthesis of AgCl-NPs by plant extracts, including *Onosma dichroantha*, *Juglans regia* and *Cissus quadrangularis*, as well as by bacteria [17-20].

The components present in the rosemary leaf extract might be considered as the source of chloride in the reaction solution for the formation of Ag/AgCl-NPs [18-20].

In order to characterize the synthesized NPs in more details, FTIR analysis of Ag/AgCl-NPs was performed and the data are shown in Figure 1d. The FTIR spectra indicate the non-bond chemical interactions between rosemary leaf extract and synthesized NPs. According to our data, sharp peaks indicative of proteins or other components attached to the synthesized nanoparticles were not detected, probably because the resulting pellet was thoroughly washed two times with distilled water before FTIR. The broad absorption bands appeared at about 3433 and 1610 cm<sup>-1</sup> are proposed to be related to the O-H stretching vibrations of the water molecules absorbed by the sample or KBr [21, 22].

In order to understand the ability of leaf extracts prepared in various seasons of a year, total NPs synthesis activity of each extract was determined by calculating the area under the UV-Vis spectrum curve. As shown in Figure 2, extracts of plants harvested in July and February with the highest total reducing capacity, were more potent in Ag/AgCl-NPs biosynthesis, whereas extracts of February and March with lower total reducing capacity showed less biosynthesis rate of Ag/AgCl-NPs. These differences could be related to the changes of

their extract components, which act in Ag<sup>+</sup> reduction. A significant correlation was observed between total phenolic and flavonoid contents, as well as between the ascorbic acid and antioxidant activity in the time course of the experiment. Changes in antioxidant capacity percentage were comparable to those of NPs biosynthesis activity (Table 1), suggesting that antioxidant capacity of Rosemary leaves play an important role in NPs biosynthesis [8]. The reduction of Ag<sup>+</sup> to Ag<sup>0</sup> is based on the chemical reduction caused by reducing and stabilizing agents present in the plant extracts; such as proteins [23], which cap the NPs and prevent aggregation [24] providing more surface availability and effective function.

**Table 1.** Correlation coefficients between antioxidant content and protein content with Ag/AgCl-NPs biosynthesis capacity.

	Under Peak Area (300 min)	Peak High (300 min)
FRAP	0.620**	0.624**
DPPH	0.381*	0.375*
Ascorbic Acid	-0.251	-0.289
Phenol	0.291	0.288
Flavonoid	0.361*	0.358*
Anthocyanin	0.175	0.163
Soluble Sugar	-0.104	-0.107
Protein	0.484**	0.482**

\*\* Correlation is significant at the 0.01 level. \* Correlation is significant at the 0.05 level.

The antibacterial tests revealed that biosynthesized NPs have significant antibacterial activity against *E. coli* and *S. aureus* clinical isolates. Ag/AgCl-NPs are gaining their importance due to their antimicrobial activities. In this study, the antibacterial effects of biosynthesized Ag/AgCl-NPs were investigated against *E. coli* and *S. aureus*. Our results indicate that biosynthesized Ag/AgCl-NPs exhibited significant antibacterial activity against two clinical bacterial isolates. In addition, leaf extracts of rosemary also exhibit a slight antibacterial effect against tested microorganism (Table 2 and Figure 3).

Recently, the synthesis of stable and monodispersive Ag-protein (core-shell) NPs using the fungal culture was approved and its effective antimicrobial potency was described against two representative bacteria, *Staphylococcus aureus* and *Klebsiella pneumonia* [24]. In another study, the protein capped Ag-NPs were prepared by fungal extract of *Coriolus versicolor* [25].

**Table 2:** Mean of inhibition zone of synthesized Ag/AgCl-NPs against *E. coli* and *S. aureus*.

Test bacterium	Treatment	Zone of inhibition (mm)
<i>E. coli</i>	Control	0 ± 0.0
	Extract (%1)	8.2 ± 0.2
	Ag/AgCl-NPs*	12.2 ± 0.4
<i>S. aureus</i>	Control	0 ± 0.0
	Extract (%1)	6.8 ± 0.1
	Ag/AgCl-NPs*	10.6 ± 0.3

\*(30 µg)

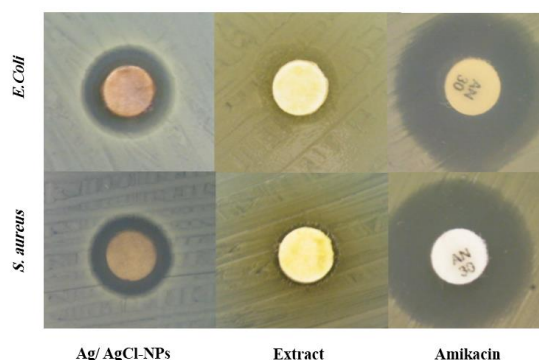


**Figure 3:** Antibacterial activity of extract (%1), biosynthesized Ag/AgCl-NPs (30 µg) and Amikacin (30 µg) against *E. coli* and *S. aureus* evaluated by the disk diffusion method.

µg) and Amikacin (30 µg) against *E. coli* and *S. aureus* evaluated by the disk diffusion method.

#### 4- CONCLUSION

Our results suggest that major constituents of Rosemary leaf extract with antioxidant activity may be the main agents in reducing Ag<sup>+</sup> ions into Ag nanoparticles. These results also indicated that leaf proteins of this species could effectively serve as the reducing and capping materials, which prevent aggregation of nanoparticles. The results can be used for standardization of plant materials harvested throughout the year, and for establishment of proper recommendations for the best harvesting time of the plant in order to gain maximum Ag-conjugated NPs. More plant species need to be evaluated for their antioxidant activity and protein content to explore the power of green and eco-friendly synthesis of metallic nanoparticles.

#### ACKNOWLEDGMENT

The authors are grateful to R. Mazandarani for help in antibacterial tests and Dr. H. R. Sadeghipour for thoroughly reading the manuscript and Dr. A. Dehno Khalaji for scientific discussion. This research was supported financially by Golestan University in the form of a grant (41.5745) awarded to MBBN.

#### REFERENCES

1. Wijnhoven, S. W., Peijnenburg, W. J., Herberts, C. A., Hagens, W. I., Oomen, A. G., Heugens, E. H., Roszek, B., Bisschops, J., Gosens, I., Van De Meent, D. (2009). "Nano-silver—a review of available data and knowledge gaps in human and environmental risk assessment", *Nanotoxicology*, 3: 109-138.
2. Mohammadinejad, R., Pourseyedi, S., Baghizadeh, A., Ranjbar, S., Mansoori, G.A. (2013). "Synthesis of Silver Nanoparticles Using *Silybum Marianum* Seed Extract", *Int. J. Nanosci. Nanotechnol.*, 9: 221-226.
3. Khatami, M., Soltani Nejad, M., Pourseyedi, S. (2015). "Biogenic Synthesis of Silver Nanoparticles Using Mustard and Its Characterization", *Int. J. Nanosci. Nanotechnol.*, 11: 281-288.
4. Shams, S., Pourseyedi, S., Hashemipour Rafsanjani, H. (2014). "Green Synthesis of Silver Nanoparticles and Its Effect on Total Proteins in *Melia Azedarach* Plant", *Int. J. Nanosci. Nanotechnol.*, 10: 181-186.
5. Shams, S., Pourseyedi, S., Hashemipour Rafsanjani, H. (2014). "Green Synthesis of Silver Nanoparticles: Eco-Friendly and Antibacterial", *Int. J. Nanosci. Nanotechnol.*, 10: 127-132

6. Ghaedi, M., Yousefinejad, M., Safarpour, M., Khafri, H.Z., Purkait, M. K. (2015). "Rosmarinus officinalis L. leaf extract mediated green synthesis of silver nanoparticles and investigation of its antimicrobial properties", *Journal of Industrial and Engineering Chemistry*, 31: 167-172.
7. Fierascu, I. C., Bunghez, I. R., Somoghi, R., Fierascu, I., Ion, R. M. (2014). "Characterization of silver nanoparticles obtained by using *Rosmarinus officinalis* extract and their antioxidant activity", *Rev. Roum. Chim*, 59: 213-218.
8. Goodarzi, V., Zamani, H., Bajuli, L., Moradshahi, A. (2014). "Evaluation of antioxidant potential and reduction capacity of some plant extracts in silver nanoparticle synthesis", *Molecular Biology Research Communications*, 3: 165-174.
9. Benzie, I., Strain, J. (1999). "Ferric reducing (antioxidant) power as a measure of antioxidant capacity: the FRAP assay", *Methods in enzymology*, 299: 15-27.
10. Cuendet, M., Hostettmann, K., Potterat, O. (1997). "Iridoid glucosides with free radical scavenging properties from *Fagraea blumei*", *Helvetica Chimica Acta*, 80: 1144-1152.
11. Meda, A., Lamien, C. E., Romito, M., Millogo, J., Nacoulma, O. G. (2005). "Determination of the total phenolic, flavonoid and proline contents in Burkina Faso honey, as well as their radical scavenging activity", *Food chemistry*, 91: 571-577.
12. Chang, C-C., Yang, M-H., Wen, H-M., Chern, J-C. (2002). "Estimation of total flavonoid content in propolis by two complementary colorimetric methods", *Journal of food and drug analysis*, 10.
13. De Pinto, M., Francis, D., De Gara, L. (1999). "The redox state of the ascorbate-dehydroascorbate pair as a specific sensor of cell division in tobacco BY-2 cells", *Protoplasma*, 209: 90-97.
14. Mita, S., Murano, N., Akaike, M., Nakamura, K. (1997). "Mutants of *Arabidopsis thaliana* with pleiotropic effects on the expression of the gene for  $\beta$ -amylase and on the accumulation of anthocyanin that are inducible by sugars", *The Plant Journal*, 11: 841-851.
15. Kochert, G. (1978). "Carbohydrate determination by the phenol-sulfuric acid method", *Handbook of phycological methods*, 2: 95-97.
16. Bradford, M. M. (1976). "A rapid and sensitive method for the quantitation of microgram quantities of protein utilizing the principle of protein-dye binding", *Analytical biochemistry*, 72: 248-254.
17. Nezamdoost, T., Bagherieh-Najjar, M. B., Aghdasi, M. (2014). "Biogenic synthesis of stable bioactive silver chloride nanoparticles using *Onosma dichroantha* Boiss. root extract", *Materials Letters*, 137: 225-228.
18. Liu, C., Yang, D., Wang, Y. (2012). "Fabrication of antimicrobial bacterial cellulose Ag/AgCl nanocomposite using bacteria as versatile biofactory", *J Nanoparticle Res*, 14: 1-12.
19. Gopinath, V., Priyadarshini, S., Meera Priyadarshini, N. (2013). "Biogenic synthesis of antibacterial silver chloride nanoparticles using leaf extracts of *Cissus quadrangularis* Linn", *Mater Lett*, 91: 224-227.
20. Kohan Baghkeirati, E., Bagherieh-Najjar, M. B., Khandan Fadafan, H., Abdolzadeh, A. (2015). "Synthesis and antibacterial activity of stable bio-conjugated nanoparticles mediated by walnut (*Juglans regia*) green husk extract", *Journal of Experimental Nanoscience*, 1-6.
21. Khansari, A., Enhessari, M., Salavati-Niasari, M. (2013). "Synthesis and Characterization of Nickel Oxide Nanoparticles from Ni(salen) as Precursor", *Journal of Cluster Science*, 24: 289-297.
22. Farhadi, S., Roostaei-Zaniyani, Z. (2011). "Simple and low-temperature synthesis of NiO nanoparticles through solid-state thermal decomposition of the hexa(ammine)Ni(II) nitrate,  $[\text{Ni}(\text{NH}_3)_6](\text{NO}_3)_2$  complex", *Polyhedron*, 30: 1244-1249.
23. Gholami-Shabani, M., Shams-Ghahfarokhi, M., Gholami-Shabani, Z., Akbarzadeh, A., Riazi, G., Razzaghi-Abyaneh, M. (2016). "Biogenic Approach using Sheep Milk for the Synthesis of Platinum Nanoparticles: The Role of Milk Protein in Platinum Reduction and Stabilization", *Int. J. Nanosci. Nanotechnol*, 12: 199-206.
24. Chowdhury, S., Basu, A., Kundu, S. (2014). "Green synthesis of protein capped silver nanoparticles from phytopathogenic fungus *Macrophomina phaseolina* (Tassi) Goid with antimicrobial properties against multidrug-resistant bacteria", *Nanoscale research letters*, 9: 365.
25. Fran cedil ois EraM, Marcelle, L. S., Cecile, O. E., Agnes, A. N., Djiopang, Y. S., Fanny, A. E. M., Lidwine, N., Harouna, M., Emmanuel, M. M. (2016). "Unexplored vegetal green synthesis of silver nanoparticles: A preliminary study with *Corchorus olitorus* Linn and *Ipomea batatas* (L.) Lam", *African Journal of Biotechnology*, 15: 341-349.